

Ga segregation and the effect of Si and Ge interlayers at the GaAs(100)/AlAs heterostructure

R. Kohleick, A. Förster, and H. Lüth

Institut für Schicht- und Ionentechnik (ISI), Forschungszentrum Jülich GmbH, P.O. Box 1913, D-52425 Jülich, Germany

(Received 29 March 1993; revised manuscript received 2 August 1993)

High-resolution ultraviolet photoemission spectra portray substantial variations in Ga 3*d* core-level line shapes, which cannot be resolved by standard x-ray-photoemission-spectroscopy techniques. They indicate that the GaAs(100)/AlAs heterointerface grown by molecular-beam epitaxy possesses a complex microstructure that is severely influenced by Ga segregation into the AlAs overlayer. The reported segregation process is highly temperature dependent and is characterized by a segregation energy of $E_s = 0.15 \pm 0.1$ eV at a substrate temperature of 630 °C. Si and Ge interlayers not only induce significant changes in the interfacial electronic structure but also effectively suppress the observed Ga segregation. Temperature-dependent measurements indicate that these structural changes do not cause the observed variations of core-level binding-energy differences and, thus, ΔE_v variations induced by group-IV interlayers.

I. INTRODUCTION

Because of their present and potential future applications in high-speed III-V-based microelectronics¹ and the apparent controllability of heterojunction band discontinuities by the insertion of group-IV interlayers,² GaAs(100)/AlAs heterojunctions have attracted considerable interest. However, despite considerable experimental^{1,3-6} and theoretical^{7,8} efforts, the atomic-scale morphology of molecular-beam-epitaxy (MBE)-grown GaAs(100)/AlAs heterointerfaces—let alone of those containing Si or Ge interlayers—is still controversial^{9,10} and remains to be clarified.

We report here on high-resolution photoemission measurements which give direct evidence for Ga segregation at GaAs(100)/AlAs heterostructures. Segregation, which poses the ultimate limit to the abruptness of GaAs/AlAs heterointerfaces, is effectively suppressed by Si and Ge interlayers comparable to those used for band-offset control even at elevated growth temperatures. Thus group-IV interlayers apparently do not only induce significant changes within the interfacial electronic structure,^{2,11} but also modify the GaAs/AlAs interfacial microstructure and Ga 3*d* core-level line shapes. However, our experiments indicate that the reported changes of band offsets cannot be explained by these interlayer-induced structural modifications within the heterointerface.

II. EXPERIMENT

The experiments were performed in a stainless-steel ultrahigh-vacuum (UHV) chamber operating at base pressures of 1×10^{-10} mbar. It is equipped with a Leybold EA/200 hemispherical energy analyzer with a multichannel detector. The photoexcited electrons enter the analyzer in the direction of the sample normal and are collected with an angular acceptance of $\pm 8^\circ$. The radiation sources employed consist of a monochromatized Al *K* α x-ray gun ($h\nu = 1486.6$ eV) and a differentially pumped gas-discharge lamp operating at the He I and He

II ($h\nu = 21.2, 40.8$ eV), and the He II satellite ($h\nu = 48.37$ eV) spectral lines.¹² Judging from the width of the Au Fermi edge, the overall resolution (electrons plus photons) for the monochromatized x-ray source is 450 meV whereas the negligible He linewidths provide a total resolution of less than 100 meV with acceptable count rates for our ultraviolet photoemission-spectroscopy (UPS) spectra.

The analysis chamber is interconnected to a MBE system described elsewhere.¹ Samples are transferred *in situ* to the analysis chamber via a UHV transfer and deposition chamber which is equipped with a low-energy electron-diffraction (LEED) system. The MBE samples were grown on Si-doped GaAs(100) wafers [$n \approx (1-3.8) \times 10^{18}$ cm⁻³]. In order to avoid excessive band bending and its detrimental effects on photoemission ΔE_v measurements,¹³ the GaAs side of the heterojunction was made up of a 1000-Å Si-doped GaAs layer ($n = 1 \times 10^{17}$ cm⁻³) onto which group-IV interlayers and nominally undoped AlAs were deposited. Throughout our experiments, the GaAs buffer layer was grown at substrate temperatures of $T_{\text{sub}} = 600$ °C. After termination of GaAs growth, the substrate temperature was set to the desired value for AlAs overgrowth and allowed to stabilize in a suitable 120–300 s time interval. After completion of III-V growth, the sample was cooled under As₄ flux down to $T_{\text{sub}} = 350$ °C.

As control experiments where the AlAs overlayer was grown under As-stabilized conditions for different V/III flux ratios at low- and high-deposition temperatures indicate, our experimental results are largely independent of the flux ratio employed. We therefore consistently deposited our AlAs overlayers using identical flux ratios.

While Si doping densities and hence Si fluxes were calibrated by Hall measurements on moderately doped samples, GaAs and AlAs growth rates were determined by monitoring reflection high-energy electron-diffraction (RHEED) intensity oscillations. Whereas Si interlayers were deposited in the MBE system according to the standard δ -doping methodology (maintaining As₄ flux while

closing group-III shutters) at $T_{\text{sub}} = 600^\circ\text{C}$, the Ge interlayers were deposited from electron-beam evaporators in a separate deposition chamber within the UHV system. Epitaxial Ge films were grown at $T_{\text{sub}} = 320^\circ\text{C}$ (Ref. 14) and layer thicknesses were monitored by a quartz crystal oscillator which was calibrated by a profilometer. Due to the comparably low substrate temperatures during Ge deposition, no stabilizing As_4 flux was supplied. After termination of Ge growth, the samples were transferred back to the MBE system for AlAs overgrowth.

Upon transfer of the III/V or group-IV covered samples into the analysis chamber, no contaminations could be detected with x-ray photoemission spectroscopy (XPS).

III. RESULTS AND DISCUSSION

A. Ga 3d core-level line shapes

Figure 1 shows Ga 3d core levels from GaAs/AlAs heterostructures processed with different AlAs growth temperatures and the Ga 3d core level of the GaAs(100) $c(4\times 4)$ surface. The spectra were taken with the He II satellite line ($h\nu = 48.37$, $E_{\text{kin}} \approx 30$ eV) and are superim-

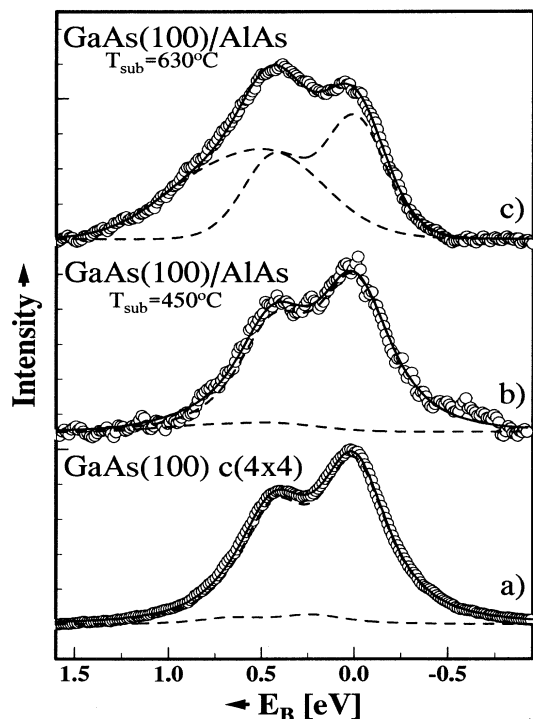


FIG. 1. Spectra of Ga 3d core levels ($h\nu = 48.37$ eV) after background subtraction. In order to compensate for variations in band bending and work function the spectra were aligned along the Ga 3d bulk core level which was taken as the zero of the binding-energy scale. Broken lines represent the different Ga 3d contributions whereas the solid lines represent the fitting results. (a) GaAs(100) $c(4\times 4)$ substrate surface; (b) GaAs(100)/5 ML AlAs grown at $T_{\text{sub}} = 450^\circ\text{C}$; (c) GaAs(100)/4 ML AlAs grown at $T_{\text{sub}} = 630^\circ\text{C}$.

posed on a smooth, featureless background. We emphasize that these spectra neither contain contributions excited by the 51.01-eV He II line, which can be found about 3 eV towards higher kinetic energies, nor distinct spectral features originating from the AlAs epilayer. This was checked by recording a similar spectrum of a 200-Å-thick, AlAs layer which was entirely featureless within the energy range shown here. Both the GaAs substrate surface and the AlAs-covered surface grown at 630°C exhibited a sharp $c(4\times 4)$ reconstruction whereas the sample in Fig. 1(b) produced a rather diffuse (2×1) reconstruction.

After subtraction of the slowly varying background, which was approximated by a third-order polynomial, we performed a line-shape analysis by modeling a set of two Ga 3d doublets to our spectra. Each spin-orbit split Ga 3d component was represented by a symmetric line shape containing both Gaussian and Lorentzian contributions.¹⁵ For the individual Ga 3d doublet, we assumed a constant spin-orbit split of 0.44 eV and an intensity ratio of 3:2 for the Ga $3d_{5/2}$ and Ga $3d_{3/2}$ lines which were assumed to have identical shapes. The lineshapes for the two doublets were allowed to vary within the fitting routine.

With this simple model, the fitting results shown in Fig. 1 are obtained. Spectra 1(a) and 1(b) can successfully be approximated by combining a high-intensity Ga 3d component with a less intense Ga 3d doublet ($\approx 6\%$ of total Ga 3d intensity) shifted about 220 (a) and 430 meV (b) towards higher binding energies. The line shapes we found for the dominant Ga 3d core lines, for both the GaAs(100) surface and the GaAs/AlAs heterostructure grown at 450°C , are strikingly similar and differ only by 20 meV in half-width [0.43 eV vs 0.45 eV for (a) and (b), respectively]. Since our experimental resolution exceeds the expected core-level lifetime broadening, both doublets have equally similar, predominantly Lorentzian shapes. We consider these to be the bulk GaAs contributions.

While it is more difficult to assign the high binding-energy component of spectrum 1(b), which is broadened by about 130 meV and contains significantly larger Gaussian contributions as compared to the corresponding Ga 3d bulk component, the high binding-energy line in spectrum 1(a) appears to originate from contributions characteristic of the As-rich $c(4\times 4)$ reconstruction of the GaAs(100) substrate surface. Both the direction of its shift and its rather low intensity compare favorably with data from literature.^{16,17}

In contrast to spectrum 1(a), the Ga 3d spectrum of the GaAs/AlAs heterostructure grown at 630°C , Fig. 1(c) can be explained by combining one Ga 3d substrate line and a second line of nearly identical intensity shifted by 0.4 eV towards higher binding energies. This second component is significantly broadened (half-width: 0.65 eV) and has a Gaussian shape with only little Lorentzian admixture. Except for its significantly lower intensity, the shifted Ga 3d component of Fig. 1(b) closely resembles that found for spectrum 1(c) both with regard to its shape and position. It therefore appears to be caused by the same physical process.

From these data we conclude that at the

GaAs(100)/AlAs heterostructure grown at elevated substrate temperatures, non-negligible amounts of Ga are in a chemically different environment as compared to bulk GaAs. Due to the significant broadening and its Gaussian character, the Ga atoms giving rise to the shifted signal appear to occupy inequivalent lattice sites. Our spectra also indicate that the process leading to the formation of this chemically shifted species is highly temperature dependent. Due to our XPS data, we can rule out contaminations as a source for these shifts on our freshly prepared samples.

As the samples of Figs. 1(b) and 1(c) were grown under identical conditions except for the substrate temperature employed, we can rule out Ga surface “contamination” from the ambience. We therefore conclude that the experimental results can best be interpreted in terms of Ga segregation from the GaAs substrate into the AlAs layer. The observed chemical shifts of the Ga 3*d* level then correspond to Ga atoms dissolved in and on the AlAs film. The negligible intensity of the shifted signal observed for our most abrupt sample, Fig. 1(b), is thought to be caused by the comparably lower number of Al neighbors to Ga atoms on the GaAs side of the abrupt heterostructure as compared to the case of Ga dissolved in AlAs.

Ga segregation is well known for the MBE growth of $\text{Al}_x\text{Ga}_{1-x}\text{As}$ where Ga-enriched or even entirely Al-depleted surfaces have been observed.^{18–20} These results are also confirmed by our measurements on $\text{Al}_x\text{Ga}_{1-x}\text{As}$ samples for values of $x=0.9$ and $x=0.5$. A rough comparison of Al 2*p* and Ga 3*d* core-level intensities indicate that the Ga surface content of the $x=0.9$ sample is in effect in the 30% range while the $x=0.5$ sample shows no significant deviation from the bulk value. In both cases we recorded UPS spectra of the Ga 3*d* core level and obtained considerably broadened Ga 3*d* lines (as compared to bulk GaAs) with half-widths of 0.57 and 0.69 eV for $x=0.5$ and $x=0.9$, respectively (considering only one Ga 3*d* doublet). This observation is consistent with our explanation of line-shape broadening due to Ga atoms situated at inequivalent lattice sites in the $\text{Al}_x\text{Ga}_{1-x}\text{As}$ alloy.

B. Coverage dependence of the Ga 3*d* signal

The behavior of this chemically shifted Ga component was further investigated by taking Ga 3*d* spectra of several GaAs(100)/AlAs heterostructures grown at a substrate temperature of 630°C with AlAs overlayer thicknesses ranging from 0.7 Å [0.25 monolayer (ML)] to 33.6 Å (12 ML). In order to prevent variations of photon flux, great care was taken to operate the discharge source with an identical set of parameters for discharge current and pressure.

The intensities found in this set of experiments are shown in Fig. 2. In all cases we assumed a half-width of 0.45 eV and a highly Lorentzian shape for the Ga 3*d* bulk level. While its shape was held constant, the line shape of the shifted component was allowed to vary freely during the fit. Consistently we obtained broad, strongly Gaussian lines, shifted by ≈ 0.4 eV towards higher binding energy. Expectedly, the Ga 3*d* bulk signal is attenuated ex-

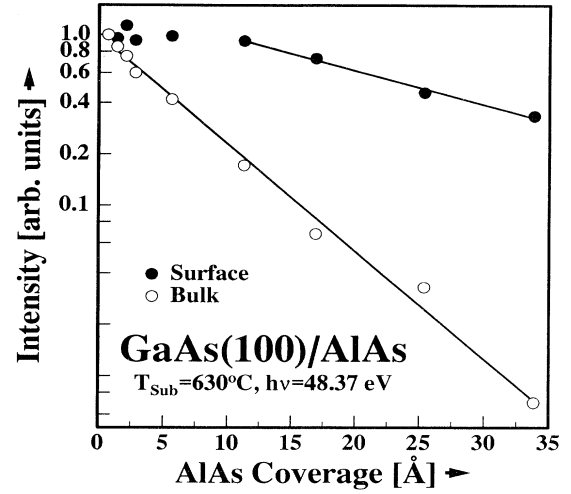


FIG. 2. Intensity of Ga 3*d* surface and bulk components of GaAs(100)/AlAs heterostructures grown at $T_{\text{sub}}=630^\circ\text{C}$ as a function of AlAs overlayer thickness.

ponentially with an escape depth of $\lambda \approx 6.8$ Å. In contrast, the intensity of the high binding-energy surface component remains at its initial value up to AlAs coverages of 15 Å. Above this coverage, the surface signal is attenuated according to an exponential law with a characteristic length of ≈ 22 Å. All our samples produced a $c(4 \times 4)$ reconstruction. However, for higher coverages exceeding 20 Å, the quality of the LEED patterns gradually deteriorated. The 200-Å AlAs layer mentioned above only produced a rather diffuse (1×1) pattern.

Assuming that Ga segregation is solely caused by an exchange reaction between the surface monolayer and the next AlAs layer, and that the surface reaches local thermodynamic equilibrium during MBE growth, we employed a simple segregation model to account for the observed intensity variation of the shifted Ga component. In this model, the segregation process is characterized by a single, phenomenological segregation energy, E_s , which is related to surface and bulk concentrations, x_s , x_b , via the following relation:²¹

$$\frac{x_s(1-x_b)}{x_b(1-x_s)} = \exp(E_s/kT). \quad (1)$$

In addition, as no Ga flux is supplied during AlAs growth, mass conservation requires that Ga of the surface layer, x_s , either segregates into the next monolayer being formed, x'_s , or remains in its position and must then be denoted as bulk material, x'_b , hence $x_s = x'_b + x'_s$. For low x_s , these two relations can be combined to yield $x'_s = \sigma x_s$, where σ is the segregation efficiency.²² This relation describes an exponential tail of Ga (in our samples about 0.25 ML in toto) distributed in the AlAs layer: $x_b(x) \propto \exp(-x/\tau)$. The remaining Ga floats on the AlAs surface: $x_s(h) \propto \exp(-h/\tau)$. The characteristic length, τ , is related to the segregation efficiency by $\tau = -(a_0/2)/\ln\sigma$, $a_0 = 5.64$ Å.

Taking this Ga distribution as an input, we calculated

the expected UPS core-level intensities for the segregated Ga atoms as a function of AIAs overlayer thickness. For high AIAs coverages ($\geq 15 \text{ \AA}$ for our value of $\lambda = 6.8 \text{ \AA}$), it is attenuated by an exponential law with a characteristic length of τ . Taking the data presented in Fig. 2, we identify $\tau \approx 22 \text{ \AA}$ which leads to a segregation efficiency of 88% and $E_s = 0.15 \pm 0.10 \text{ eV}$ in good quantitative agreement with the value of $0.1 \pm 0.05 \text{ eV}$ reported by Moison *et al.*²² from XPS and Auger electron spectroscopy (AES) measurements on $\text{Al}_x\text{Ga}_{1-x}\text{As}$ alloys.

We assume that the observed Ga segregation and chemical shifts are somehow linked to the As-rich $c(4 \times 4)$ surface reconstruction observed for our thin high-temperature AIAs overlayers on GaAs and also thick $\text{Al}_x\text{Ga}_{1-x}\text{As}$ layers grown by MBE. It is known from literature^{23,24} and also confirmed by our own observation for 200- \AA AIAs overlayers that the $c(4 \times 4)$ reconstruction cannot be produced for bulk-like, i.e., thick AIAs(100) layers on GaAs. Both the slow deterioration of our LEED patterns for higher coverages—where the surface Ga content has already been reduced decisively—and the (2×1) pattern observed for the low-temperature AIAs layer of Fig. 1(b)—where only negligible amounts of segregated material are observed—support this hypothesis.

C. Si and Ge interlayers

Figure 3 shows spectra of the Ga $3d$ core level for samples with 0.5-ML (1ML = $6.25 \times 10^{14} \text{ atoms/cm}^2$) Ge (b) and Si (c) interlayers embedded in GaAs(100)/3 ML AIAs heterostructures. For a comparison the spectrum of Fig. 1(c) is also reproduced in Fig. 3(a). In all cases the AIAs growth temperature was 630°C . For sample 3(c) these growth conditions correspond to the methodology employed in Ref. 2. With monochromatized XPS, we also measure large $\approx 0.4 \text{ eV}$ changes in the Ga $3d$ and Al $2p$ core-level separation for the Si interlayer, whereas the effect of the Ge interlayer on core-level separation is reduced to 0.15 eV presumably through Ge diffusion at our high growth temperatures.

As samples where both Ge interlayer and AIAs overlayer were grown at a substrate temperature of 320°C equally show $\approx 0.4 \text{ eV}$ changes of the Al $2p$ –Ga $3d$ core-level separation, we conclude that the difference in binding energies between samples containing Si and Ge interlayers processed at elevated growth temperatures is not caused by the different growth techniques employed (Si: MBE; Ge: *e* beam) but rather due to non-negligible Ge diffusion at these comparably high deposition temperatures.

The line shapes found for spectra 3(b) and 3(c) differ decisively from those found for spectrum 3(a) even though the AIAs overlayers were processed at the same growth temperature. They can only be modeled by assuming a combination of a broad [half-width: 0.59 eV and 0.55 eV for (b) and (c) respectively], high-intensity peak with a strong Lorentzian shape and a weak (7% of total Ga $3d$ intensity for Si and 19% for Ge interlayers), Gaussian peak shifted about 0.45 eV (Ge) and 0.39 eV (Si) towards lower binding energies. It is also broadened

significantly with regard to the Ga $3d$ bulk level [half-width: 0.88 eV and 0.53 eV for (b) and (c), respectively]. For our growth conditions, sample 3(b) (Ge) produced a rather diffuse (2×1) LEED pattern, whereas sample (c) (Si) exhibited a slightly better (2×1) reconstruction. Again, the absence of the high binding-energy Ga $3d$ component coincides with the disappearance of the $c(4 \times 4)$ reconstruction observed for our high-temperature GaAs/AIAs samples without interlayers.

Earlier reports indicate that Si δ -doping may lead to bulk concentrations of up to $4 \times 10^{19} \text{ cm}^{-3}$.²⁵ The strong band-bending associated with such a high dopant density, which may well lie in the range of our escape depth of 6.8 \AA , could lead to a significant broadening of the observed core-level lines. In our experiments, we do observe a significant broadening of the Ga $3d$ core level on the order of $\approx 100 \text{ meV}$ as compared to bulk GaAs. However, due to the extreme dopant concentrations, structural and electronic changes in the environment of Ga atoms induced by the group-IV interlayer should also be considered as possible reasons contributing to the observed line-shape broadening.

Structural reasons are also supported by the x-ray photoelectron diffraction investigation undertaken by Chambers and Loebs⁹ for GaAs(001)/1 ML Si structures grown at $T_{\text{sub}} = 450^\circ\text{C}$. They observe substitutional Si in

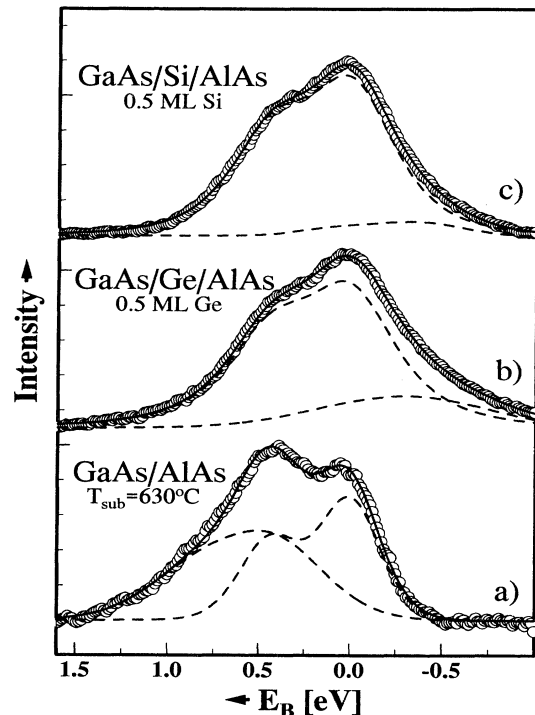


FIG. 3. Spectra of Ga $3d$ core levels ($h\nu = 48.37 \text{ eV}$) after background subtraction. The alignment corresponds to that of Fig. 1. Again, broken lines represent the different Ga $3d$ contributions whereas the solid lines represent the fitting results. (a) GaAs(100)/4 ML AIAs as in Fig. 1(c); (b) GaAs(100)/0.5 ML Ge/3 ML AIAs; (c) GaAs(100)/0.5 ML Si/3 ML AIAs. In all cases the AIAs overlayers were grown at $T_{\text{sub}} = 630^\circ\text{C}$.

the first three atomic layers of the GaAs surface and associate the (2×1) reconstruction with Si atoms displaced from GaAs bulk coordinates. It is therefore tempting to associate the line-shape broadening either with disorder induced by Si located at substitutional sites or a reduction of core-hole lifetime due to a substantial increase in electron density supplied by Si and Ge donors or a combination of both. The additional low binding-energy component is thought to indicate the formation of Si-Ga bonds with Ga acting as an acceptor of charge. Taking into consideration the higher diffusivity of Ge in GaAs the same reasoning should apply for spectrum 3(b) only but with an increased number of Ge-Ga bonds.

However, it is obvious from our spectra that in contrast to spectrum 3(a) the high binding-energy line associated to the segregated Ga component is not present in the samples grown with group-IV interlayer. Therefore we conclude that Ga segregation is effectively suppressed both by Si and Ge interlayers.

The apparent suppression of Ga segregation by the interlayers cannot readily be explained by our data. Possible reasons might include simple structural processes as lattice sites otherwise accessible to Ga during the segregation process are occupied by Si and Ge interlayer atoms. In addition to that, one might also envisage a segregation barrier induced by the space charge of electrically active Si and Ge atoms acting as n -type dopants. Similar to the field-induced migration of Si dopants in GaAs (Ref. 26) where positively charged Si ions are driven by surface-pinning induced fields, the downward band bending associated with any strong N^- -type doping might act as a barrier for slightly positive Ga cores. As our value of 150 meV for E_s indicates, the absolute magnitude of this barrier need not necessarily be high.

D. Influence of Ga segregation on band offset

Group-IV interlayers in the GaAs(100)/AlAs heterostructure do not only induce significant changes in core-level binding-energy differences which can be associated with changes in ΔE_v ,² but they also suppress Ga segregation into the AlAs overlayer. In order to investigate whether this correlation between changes in atomic microstructure and electronic properties is significant or purely accidental, we measured variations of the interface dipole for GaAs(100)/AlAs heterostructures deposited at varying AlAs growth temperatures and consequently varying amounts of segregated Ga.

In order to determine variations of the interface dipole, we measured the Ga $3d_{5/2}$ to Al $2p_{3/2}$ binding-energy differences by monochromatized XPS and the bulk Ga $3d_{5/2}$ to AlAs valence-band maximum (VBM) binding-energy difference by UPS. Al $2p_{3/2}$ and Ga $3d_{5/2}$ core-level positions were determined by fitting appropriate doublets to the measured Al $2p$ and Ga $3d$ XPS core-level line shapes. The valence-band maximum was approximated by fitting a linear function broadened by the experimental resolution to our spectra. Changes of both binding-energy differences indicate modifications of the heterostructure interface dipole and hence ΔE_v . As we employed two different photon energies with associated

different escape depths and also different spectral features, we can rule out artifacts due to band-bending changes. While our UPS measurements take into account line-shape variations of Ga $3d$ core level, they cannot be detected by monochromatized XPS due to its low surface sensitivity ($\lambda \approx 25$ Å) and its poor resolution. Consequently, the XPS Ga $3d$ line shape does not vary significantly in our experiments. As our results indicate, the Al $2p$ level line shape does not vary decisively with AlAs growth temperature.

The data presented in Fig. 4 were measured on GaAs(100)/5 ML AlAs heterostructures deposited at different AlAs growth temperatures. Our data show that the interface dipole and ΔE_v do not vary with AlAs growth temperature and therefore do not depend on the amount of segregated Ga. These findings support theoretical work by Baroni *et al.*²⁷ which states that at lattice-matched heterostructures sharing a common anion, the band discontinuities are independent of any linear and isovalent (here Ga-Al swaps) modification of the heterointerface.

As the interface dipole of the GaAs(100)/AlAs heterostructure does not depend on the Ga distribution at the heterointerface, we conclude that the interlayer-induced modifications of the Ga distribution at the heterointerface do not contribute significantly to the observed modifications of the interfacial electronic structure, i.e., changes in ΔE_v .

IV. CONCLUSION

Our measurements show that standard XPS techniques do not provide sufficient resolution to fully characterize the GaAs(100)/AlAs heterostructure. Our high-

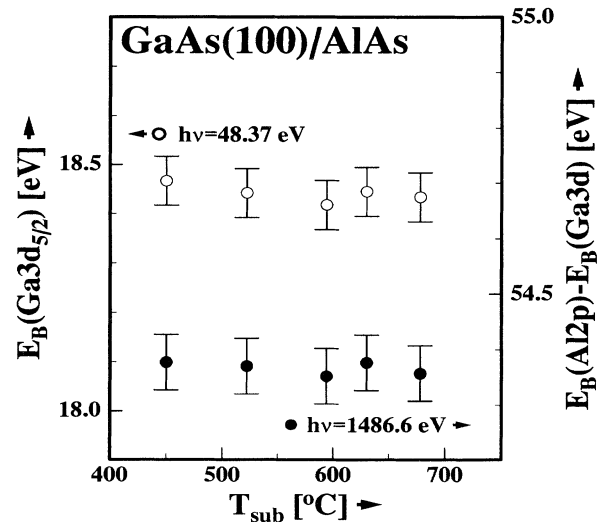


FIG. 4. Variation of Ga $3d$ to Al $2p$ and Ga $3d$ to VBM (AlAs) binding energy difference as measured with monochromatized XPS ($h\nu=1486.6$ eV) and UPS ($h\nu=48.37$ eV) on GaAs(100)/5 ML AlAs heterostructures for different AlAs growth temperatures. Any variation of the interface dipole or the band offset, ΔE_v , should manifest themselves as variations in the values shown here.

resolution UPS measurements indicate that the GaAs(100)/AlAs heterointerface possesses a complex microstructure which is significantly influenced by Ga segregation into the AlAs overlayer. Apart from the well-known monolayer-sized steps found for MBE-grown samples, segregation poses an additional limitation on the abruptness of the GaAs/AlAs heterointerface and, consequently, device performance.

Contrary to previous findings,² the Ga 3d core-level line shape is severely affected by the presence of Si and Ge interlayers at the heterointerface. The underlying reason is a subtle modification of the Ga distribution within the heterostructure as Ga segregation is suppressed by both Si and Ge interlayers. This Ga redistribution, however, does not affect the band alignment across the heterojunction.

It remains to be seen whether similar modifications of core-level line shapes induced by group-IV interlayers

can also be observed—possibly by high-resolution synchrotron radiation studies—for the Al 2p core levels (found at binding energies of ≈ 70 eV) which are usually employed for the determination of the heterostructure band offset. Slight (≈ 100 meV) increases in Al 2p linewidth induced by Si interlayers have been reported in the literature¹⁰ and are also supported by our XPS measurements on samples with Si interlayers.

Our experiments suggest that at least for the GaAs/AlAs system even higher experimental resolution than that provided by monochromatized XPS should be employed for determining band offsets and their changes due to interlayer deposition.

ACKNOWLEDGMENT

We thank Ch. Krause for his assistance in preparing the MBE samples.

-
- ¹A. Förster, J. Lange, D. Gerthsen, C. Diecker, and H. Lüth, *J. Vac. Sci. Technol. B* **11**, 1743 (1993).
- ²L. Sorba, G. Bratina, G. Ceccone, A. Antonini, J. F. Walker, M. Micovic, and A. Franciosi, *Phys. Rev. B* **43**, 2450 (1991).
- ³A. Ourmazd, D. W. Taylor, and J. Cunningham, *Phys. Rev. Lett.* **62**, 933 (1989).
- ⁴D. Bimberg, F. Heinrichsdorff, R. K. Bauer, D. Gerthsen, D. Stenkamp, D. E. Mars, and J. N. Miller, *J. Vac. Sci. Technol. B* **10**, 1793 (1992).
- ⁵H. Sakaki, T. Noda, K. Hirakawa, M. Tanaka, and T. Matsusue, *Appl. Phys. Lett.* **51**, 1934 (1987).
- ⁶B. Jusserand, F. Mollot, J.-M. Moison, and G. Le Roux, *Appl. Phys. Lett.* **57**, 560 (1990).
- ⁷R. G. Dandrea, C. B. Duke, and A. Zunger, *J. Vac. Sci. Technol. B* **10**, 1744 (1992).
- ⁸A. Mujica, R. Pérez, F. Flores, and A. Muñoz, *Phys. Rev. B* **46**, 9641 (1992).
- ⁹S. A. Chambers and V. A. Loebis, *Phys. Rev. B* **47**, 9513 (1993), and references therein.
- ¹⁰M. Akazawa, H. Hasegawa, H. Tomozawa, and H. Fujikura, *Jpn. J. Appl. Phys.* **31**, L1012 (1992).
- ¹¹G. Bratina, L. Sorba, A. Antonini, G. Biasiol, and A. Franciosi, *Phys. Rev. B* **45**, 4528 (1992).
- ¹²J. A. R. Samson, *Techniques of Vacuum Ultraviolet Spectroscopy* (Wiley, New York, 1967).
- ¹³E. A. Kraut, R. W. Grant, J. R. Waldrop, and S. P. Kowalczyk, *Phys. Rev. B* **28**, 1965 (1983).
- ¹⁴A. D. Katnani, P. Chiaradia, H. Sang, P. Zurcher, and R. S. Bauer, *Phys. Rev. B* **31**, 2146 (1985).
- ¹⁵R. D. B. Fraser and E. Suzuki, *Anal. Chem.* **41**, 37 (1969).
- ¹⁶R. Ludeke, T.-C. Chiang, and D. E. Eastman, *Physica B* **117**, 819 (1983).
- ¹⁷A. D. Katnani, H. W. Sang, Jr., P. Chiaradia, and R. S. Bauer, *J. Vac. Sci. Technol. B* **3**, 608 (1985).
- ¹⁸T.-C. Chiang, R. Ludeke, and D. E. Eastman, *Phys. Rev. B* **25**, 6518 (1982).
- ¹⁹R. A. Stall, J. Zilko, V. Swaminathan, and N. Schumaker, *J. Vac. Sci. Technol. B* **3**, 524 (1985).
- ²⁰J. Massies, F. Turco, A. Saletes, and J. P. Contour, *J. Cryst. Growth* **80**, 307 (1987).
- ²¹*Adsorption on Metal Surfaces*, edited by J. Bénard (Elsevier, Amsterdam, 1983).
- ²²J. M. Moison, C. Guille, F. Houzay, F. Barthe, and M. Van Rompay, *Phys. Rev. B* **40**, 6149 (1989).
- ²³R. Z. Bachrach, R. S. Bauer, P. Chiaradia, and G. V. Hansson, *J. Vac. Sci. Technol.* **19**, 335 (1981).
- ²⁴W. I. Wang, *J. Vac. Sci. Technol. B* **1**, 574 (1983).
- ²⁵H. C. Nutt, R. S. Smith, M. Towers, P. K. Rees, and D. J. James, *J. Appl. Phys.* **70**, 821 (1991).
- ²⁶E. F. Schubert, J. M. Kuo, R. F. Kopf, A. S. Jordan, H. S. Luftmann, and A. S. Hopkins, *Phys. Rev. B* **42**, 1364 (1990).
- ²⁷S. Baroni, R. Resta, A. Baldereschi, and M. Peressi, in *Spectroscopy of Semiconductor Microstructures*, Vol. 206 of *NATO ASI Series B: Physics*, edited by G. Fasol, A. Fasolino, and P. Lugli (Plenum, New York, London, 1989).